Analysis of transition variables in a continuous-discontinuous model to describe the crack process in concrete structures

Lívia Ramos Santos Pereira[1], Samuel Silva Penna[2]

[1,2]*Dept. of Structural Engineering, Federal University of Minas Gerais*
Av. Antônio Carlos, 6627, 31270 – 901, MG, Brazil
[1] *lrsp@ufmg.br*, [2]*spenna@dees.ufmg.br*

Abstract. The complete characterization of fracture in quasi-brittle materials such as concrete remains a challenge in computational modeling because of the complexity of this phenomenon and the material constitution. Continuous-discontinuous approaches have been developed to fill this gap, embracing the continuous degradation process related to smeared cracks and the discontinuity representation when discrete cracks emerge. Besides the efforts, there is no consensus about the transition procedure between continuous and discontinuous. The literature indicates that many parameters can be monitored to annunciate the transition, such as energy, historical variables, crack length, crack opening, etc. But the most frequently used variable is damage. More recently, the phase-field models have shown an ability to connect Continuum Damage Mechanics and Fracture Mechanics, acting as a crack enunciator and tracker. Considering the context, an analysis of the transition variable and the value it assumes during the evolution of smeared degradation to an explicit crack is proposed. A combined strategy that associates nonlocal damage models with a mesh redefinition model based on nodal duplication is adopted. Two parameters are compared in the transition function: the damage variable and the phase-field variable. Some numerical simulations were performed, admitting different limit values. The results are analyzed to establish the optimal value that characterizes crack nucleation and which parameter works better as a transition variable.

Keywords: Continuous-discontinuous model, Fracture representation, Transition variable, Damage, Phase-field

1 Introduction

The continuous-discontinuous models have emerged to describe the complete degradation process in concrete structures, coupling smeared cracking approaches with the discrete representation of macroscopic cracks. A relevant issue in these models is the passage between the continuous and the discontinuous media, which is established by a transition variable. In this approach, the first stages of degradation are described by a continuous model until the fracture identification. Then, a discrete model assumes the function of reproducing the discontinuity.

Janson and Hult [1] had already argued for an approach combining concepts from damage and fracture. These authors considered damage a transition model capable of filling the gap between the Theory of Elasticity and fracture. Later, other studies showed the need for a formal link to attach both strategies. Legendre and Mazars [2] presented an approach associating damage with fracture following the thermodynamic laws and the equivalent crack. Mazars and Pijaudier-Cabot [3] also developed a continuous-discontinuous model from the equivalent crack. Their contribution was adopting a nonlocal damage model to describe the continuous, based on the requirement of an independent model from the mesh discretization. The transition parameter is the damage critical value, D = 1.0.

On the other hand, Jirásek and Zimmermann [4] proposed the Delayed Embedded Crack (DEC). Such a model relates a nonlocal damage model to the Embedded Finite Element Method (EFEM). The crack is called *delayed* because the initial cracks can rotate when the predicted propagation orientation is incorrect. The transition criterion adopted is the critical crack opening value. Another variation of the Finite Element Method (FEM) was introduced into the continuous-discontinuous models by Simone et al. [5]. These authors applied the eXtended Finite Element Method (XFEM) to represent cracks using the enrichment and an enhanced gradient model to regularize the continuous. The discontinuities start when damage reaches the final stage of degradation. From these methods, various continuous-discontinuous models adopting XFEM were developed [6–9].

A continuous-discontinuous model denominated Xfield, embracing a Phase-Field Model (PFM) and XFEM, was proposed by Giovanardi et al. [10]. While the XFEM is responsible for the displacement field calculus, the phase-field indicates nucleation and propagation of cracks. The crack propagation direction is determined according to the maximization of the phase-field gradient. Geelen et al. [11] also associated XFEM and phase-field. In this study, the phase-field describes the continuous as an attempt to fill the gaps in representing crack nucleation, ramification, and coalescence. The crack length function unleashes the continuous-discontinuous transition while an auxiliary damage field announces the crack path. The XFEM has the role of inserting the discontinuities into the displacement field.

Using variations of the classic FEM to reproduce fracture without interfering with the original mesh reflects a trend of preventing remeshing since this technique has a relevant computational cost. However, such models need to improve in representing the actual topology of discrete cracks. Considering the technologies available and modern computers, it is possible now to rescue models that include explicit discontinuities into the mesh.

Regarding the efforts to develop models to transit between the continuous and the discontinuous, Rabczuk [12] highlights that it remains a challenge in the computational mechanical field. Wu et al. [13] stress that there is no consensus about the connection between smeared degradation and the discrete crack, mainly when fracture conducts to media anisotropy. Because of these limitations, this study area still requires further investigation.

Based on the above, this work analyzes the transition variable and the value it assumes when the smeared degradation evolves to an explicit crack. The continuous-discontinuous model adopted couples a nonlocal damage model with a nodal duplication algorithm when the crack opening is governed by damage. When the phase-field controls the crack, an extra PFM is required. Two parameters are compared as transition variables: damage and phase-field variables. Numerical simulations are performed, varying the values of these parameters to verify the results regarding crack representation and structural response.

2 Continuous-discontinuous model

In this work, to represent the discrete fracture, a mesh redefinition model based on the nodal duplication technique is adopted. Further, a nonlocal damage model is assumed to describe the continuous degradation. The nonlocal damage model is based on the equivalent strain of de Vree et al. [14] and describes the material media response. The nodal duplication algorithm requires internal variables from the constitutive model to announce crack opening and propagation. This parameter is calculated in the current node and compared with a crack limit previously determined. If the current value exceeds the limit, a new crack opens, or an existing crack propagates. More details about the nodal duplication algorithm are described by Pereira and Penna [15].

A more general model was developed to improve the crack process description. While the PFM of Miehe et al. [16, 17] is adopted to announce crack nucleation, the nonlocal damage model remains responsible for the medium degradation.

2.1 Nonlocal damage model

The damage model developed by de Vree et al. [14] is adopted to describe the material media and calculate the damage variable (D). This model equivalent strain ($\tilde{\varepsilon}$) is given by

$$\tilde{\varepsilon} = \frac{c-1}{2c(1-2\nu)} I_1^{\varepsilon} + \frac{1}{2c}\sqrt{\left[\frac{(c-1)}{(1-2\nu)} I_1^{\varepsilon}\right]^2 + \frac{12c}{(1-\nu)^2} J_2^{\varepsilon}}, \tag{1}$$

where c is the ratio between concrete compression strength and concrete tensile strength (f_c/f_t); ν is the Poisson ratio; I_1^{ε} the first invariant of the strain tensor; J_2^{ε} is the second invariant of the deviatoric strain tensor. The invariants are calculated as

$$I_1^{\varepsilon} = \varepsilon_{kk}; \qquad J_2^{\varepsilon} = \frac{1}{2} e_{ij} e_{ij}, \quad \text{with} \quad e_{ij} = \varepsilon_{ij} - \frac{1}{3}\varepsilon_{kk}\delta_{ij}. \tag{2}$$

The strain tensor components are represented by ε_{ij}, and δ_{ij} is the Kronecker delta. The secant operator is

$$E^s_{ijkl} = (1-D) E^0_{ijkl}. \tag{3}$$

In this work, the damage parameter is obtained from an exponential law, depending on the equivalent strain

$$D(\tilde{\varepsilon}) = 1 - \frac{\kappa_0}{\tilde{\varepsilon}} \left[1 - \alpha + \alpha e^{-\beta(\tilde{\varepsilon} - \kappa_0)}\right], \tag{4}$$

with κ_0 indicating the equivalent strain associated with the damage initiation, α the maximum value of damage, and β the damage evolution intensity.

The nonlocal strategy is assumed to avoid strain localization. The integral formulation suggested by Jirásek and Zimmermann [4] is adopted, replacing the local strain (eq. (1)) by a nonlocal measure $\bar{\varepsilon}$

$$\bar{\varepsilon}(\mathbf{x}) = \frac{1}{V_r(\mathbf{x})} \int_V \alpha(\|\mathbf{s} - \mathbf{x}\|)\tilde{\varepsilon} dV, \tag{5}$$

with

$$V_r(\mathbf{x}) = \int_V \alpha(\|\mathbf{s} - \mathbf{x}\|) dV, \tag{6}$$

where $\bar{\varepsilon}$ is the nonlocal equivalent strain, V is the nonlocal domain volume, $\alpha(\mathbf{x})$ is the weighting function, and $\|\mathbf{s} - \mathbf{x}\|$ is the distance between the reference point located in $\mathbf{x}$ and a point in the neighborhood, situated in $\mathbf{s}$.

The current paper admits the weighting function as the Gaussian distribution

$$\alpha(\mathbf{x}) = -e^{(k_s|\mathbf{x}|/\ell)^2}, \tag{7}$$

with k_s controlling the shape of the function.

2.2 Phase-Field Model of Miehe et al. [16, 17]

The PFM of Miehe et al. [16, 17] was employed because of its capacity to represent cracks only in tension regions, representing better the concrete behavior. The cracks are suppressed in compression areas due to the spectral decomposition of the strain tensor, written as

$$\underline{\varepsilon} = \sum_{n=1}^{3} \varepsilon_n \bar{p}_n \otimes \bar{p}_n = \underline{\varepsilon}^+ + \underline{\varepsilon}^-, \tag{8}$$

where $\underline{\varepsilon}^+$ and $\underline{\varepsilon}^-$ are the positive (tension) and the negative (compression) components of the strain tensor

$$\underline{\varepsilon}^+ = \sum_{n=1}^{3} \langle \varepsilon_n \rangle_+ \bar{p}_n \otimes \bar{p}_n; \quad \underline{\varepsilon}^- = \sum_{n=1}^{3} \langle \varepsilon_n \rangle_- \bar{p}_n \otimes \bar{p}_n. \tag{9}$$

being ε_n and $\bar{p}_n$, in this order, the eigenvalues and eigenvectors of the strain tensor. The ramp functions $\langle x \rangle_+$ and $\langle x \rangle_-$ return the module of x if $x \geq 0$, or zero, for $x < 0$. The constitutive tensor is obtained from

$$\hat{\mathbf{C}} = g(\phi) \left[\lambda_0 R_n^+ \underline{I} \otimes \underline{I} + 2\mu_0 \hat{\mathbf{P}}^+\right] + \lambda_0 R_n^- \underline{I} \otimes \underline{I} + 2\mu_0 \hat{\mathbf{P}}^-, \tag{10}$$

where $g(\phi)$ is the degradation function; λ_0 and μ_0 are the Lamé constants; R_n^+ and R_n^- are functions to analyze the sign of the strain tensor trace (eq. (11)); $\hat{\mathbf{P}}^+$ and $\hat{\mathbf{P}}^-$ are fourth-order tensors to write the tension and compression parcels of the strain tensor (eq. (12)).

$$R_n^+ = \mathrm{H}(\mathrm{tr}(\underline{\varepsilon})); \qquad R_n^- = \mathrm{H}(-\mathrm{tr}(\underline{\varepsilon})). \tag{11}$$

$$\hat{\mathbf{P}}^+ = \sum_{n=1}^{3} \mathrm{H}(\varepsilon_n) \bar{p}_n \otimes \bar{p}_n \otimes \bar{p}_n \otimes \bar{p}_n, \qquad \hat{\mathbf{P}}^- = \mathbf{I_4} - \hat{\mathbf{P}}^+. \tag{12}$$

Function H(x) refers to the Heaviside function. The whole formulation of this PFM is available in [16, 17].

3 Transition variable

Besides some continuous-discontinuous models proposed in the literature to describe the whole fracture process, the definition of which variable should be observed to define the passage from the smeared degradation to

Table 1. Transition criteria

Author	Transition criteria	Author	Transition criteria
Legendre and Mazars [2]	energy limit (G_c)	Mazars and Pijaudier-Cabot [3]	D = 1.0
Jirásek and Zimmermann [4]	crack opening	Simone et al. [5]	damage
Mediavilla et al. [18]	damage	Comi et al. [6]	damage
Moonen et al. [7]	cohesive model	Cuvilliez et al. [19]	damage
Karamnejad et al. [8]	tensile strength	Roth et al. [9]	D = [0.6, 0.7]
Giovanardi et al. [10]	phase-field	Geelen et al. [11]	crack length

the discrete crack remains a point of discussion. Another issue is the critical value that this variable assumes in the transition instant. Table 1 summarizes relevant works in this research field, identifying the transition criteria.

Based on the above, the present work evaluates the performance of damage and phase-field as transition variables in the continuous-discontinuous approach adopted. This choice is justified by the frequent occurrence of damage as a transition parameter, as shown in Table 1, and the phase-field capacity of identifying nucleation, propagation, ramification, and coalescence of multiple crack tips. Both measures vary from zero, to undamaged material, to 1.0, which characterizes the complete degradation.

4 Numerical simulations

The experimental test of Winkler et al. [20, 21] was adopted to evaluate the behavior of the implemented model. The geometry of the specimen, the cracked area obtained by [20, 21], and the 3-node triangular finite element mesh admitted in the simulations are shown in Figure 1.

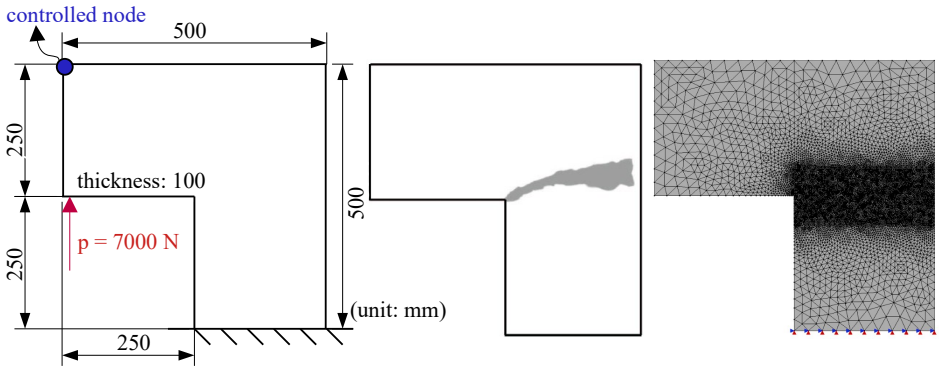

Figure 1. Crack paths announced via phase-field.

The material parameters provided in [20, 21] are: $E_0 = 25850(\pm 1381)$ N/mm^2, $f_t = 2.7$ N/mm^2, $f_c = 31.0$ N/mm^2, $G_c = 0.065$ N/mm and $\nu = 0.18$. The minimum Young modulus was adopted for a better adjustment, given as $E_0 = 24469$ N/mm^2. The concrete maximum aggregate size is $d_{max} = 8$ mm.

The nonlocal damage model based on de Vree et al. [14] requires some additional parameters, defined by fitting the damage law with the material stress-strain relation in uniaxial tension simulation: $\alpha = 0.97$, $\beta = 1000$, and $\kappa_0 = 1.35 \times 10^{-4}$. The phase-field analyses assumed the geometric crack and the energetic crack function of Bourdin et al. [22], and the length scaled was estimated as 6 mm, which represents the region of influence of the phase-field variable. The Gaussian weight function (eq. (7)) was applied, considering the constant $k_s = 1.0$ and the local ratio of $\ell = 32$ mm.

For the solution process was adopted the direct displacement control method [23] and secant equilibrium. The vertical displacement of the node highlighted in Figure 1 was controlled, with increment of 0.01 mm and convergence tolerance of 1.0×10^{-4}.

Two different analyses were performed. First, simulations were conducted to evaluate the values that best characterize the continuous-discontinuous transition using damage and phase-field. In this analysis, the crack nucleation node was prescribed. A second analysis was performed to evaluate how damage and phase-field work as crack nucleation parameters. In this case, the crack could emerge at any point in the mesh.

4.1 Analysis of the transition variable value

From the values of critical damage related in the literature, as presented in Table 1, the interval between 0.6 and 1.0 was tested in a series of numerical simulations for both damage and phase-field. In these analyses, the node where the crack initiate is located in the panel corner, according to the crack path observed in the experimental tests. The results are indicated in Figs. 2 and 3 in terms of the equilibrium path and the crack path representation.

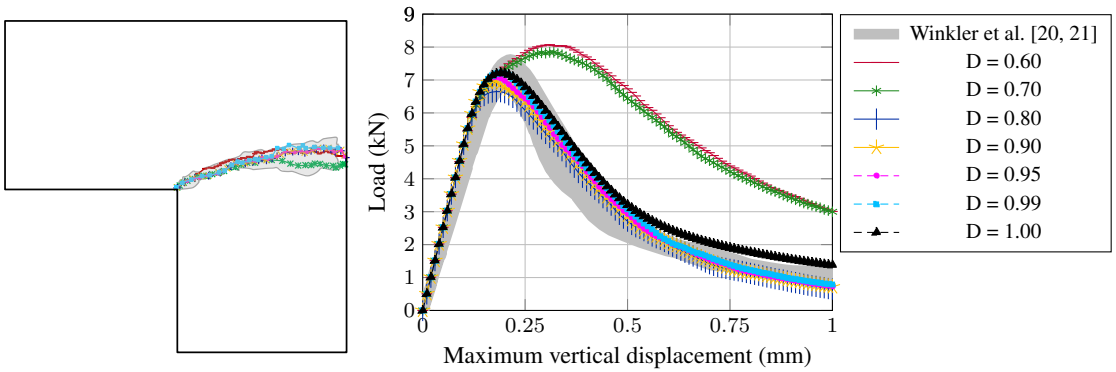

Figure 2. L-shaped panel: crack propagation by damage.

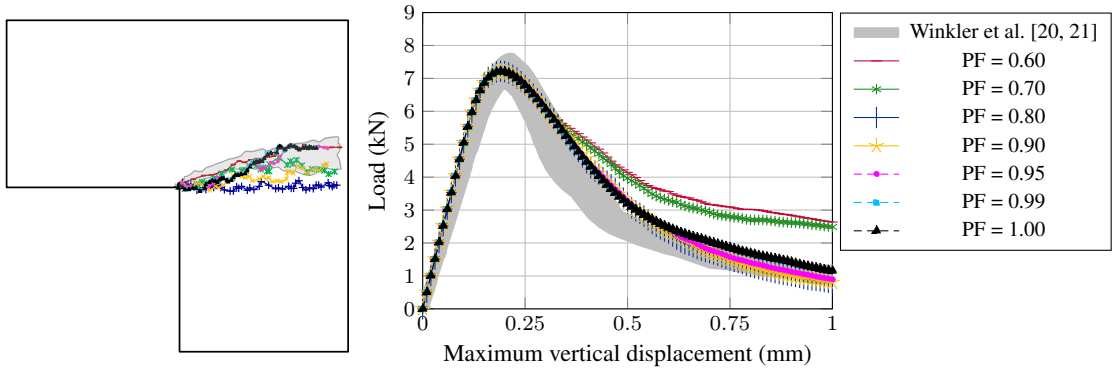

Figure 3. L-shaped panel: crack propagation by phase-field.

The damage performance (Figure 2) presented coherence with the experimental data for damage nucleation limits between 0.8 and 0.99 for the equilibrium path and also for the crack representation. Although the nucleation limits of 0.6 and 0.7 had a consistent crack representation, the peak of the equilibrium path presented an increase due to incorrect crack definition by the discontinuous strategy. This issue will be discussed in the next simulation. No crack was verified for $D = 1.0$ because the maximum damage value was not reached, which was expected since the maximum degradation of the material is $\alpha = 0.97$. In this last case, the equilibrium path is the conventional continuous behavior. In short, when damage is adopted as the transition variable, the best crack opening limits are in the interval $[0.8, 0.99]$.

The results associated with the phase-field (Figure 3) had a general behavior close to the one verified by damage, but some differences were observed. Despite the differences in the descending branch, the peak of the equilibrium path related to the crack opening limits of 0.6 and 0.7 did not change compared with the superior values of the critical phase-field. For PF = 0.8 and PF = 0.9, besides the coherent numerical curve, the crack representation did not fit so well with the degradation area observed in the experimental tests. Moreover, a good performance was achieved by admitting PF = 1.0, the maximum value allowed. Based on these observations, when the phase-field variable is considered to describe the crack, the best limit values are between 0.95 and 1.0.

4.2 Crack nucleation test

New analyses were performed considering that the crack nucleation point is the one that reaches the critical value of damage or phase-field established. The same example was used, fixing the transition limit in D = PF = 0.95. It is observed that both simulations presented a crack opening starting in the same node. However, the crack

starts early in the analysis conducted by damage. The crack representation and the equilibrium paths are illustrated in Figure 4, while it is shown in Figures 5 and 6 the deformed shape of the L-shaped panel.

Evaluating the crack representation (Figure 4), the analysis adopting critical damage as the transition variable had a better result when compared to the degradation area experimentally observed. The deviation observed in the numerical test admitting phase-field is probably related to the residual elements connecting the crack sides, as shown in Figure 6, which is not verified in Figure 5. These elements also justify the slightly greater peak and the post-peak stiffening observed in the equilibrium path associated with PF (Figure 4).

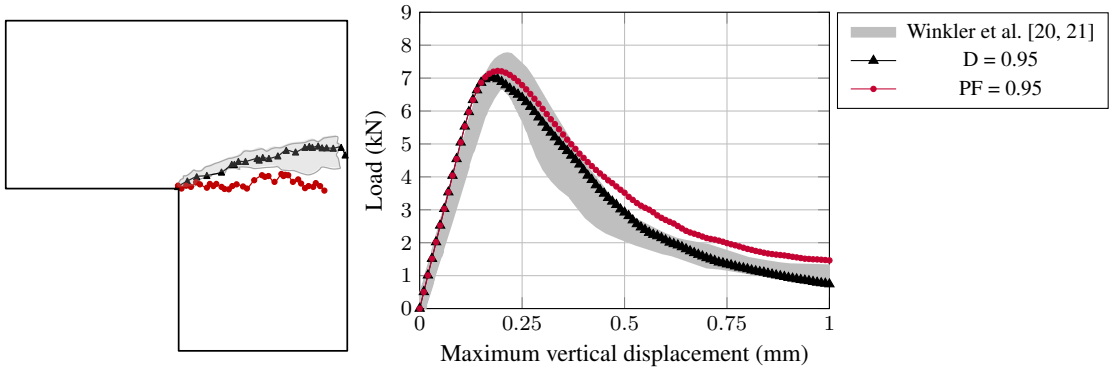

Figure 4. L-shaped panel: analysis of spontaneous nucleation.

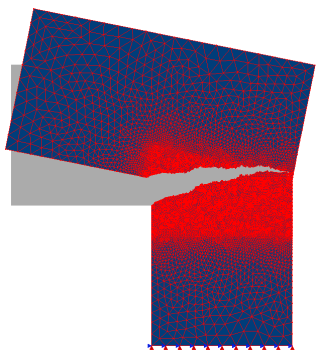

Figure 5. Deformed shape: damage analysis.

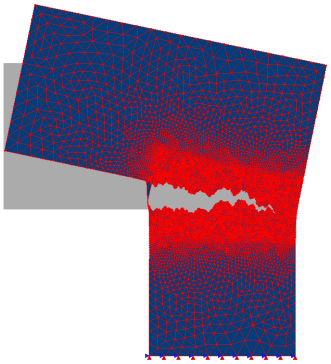

Figure 6. Deformed shape: phase-field analysis.

5 Conclusions

Based on the results, the main conclusions of the current work are summarized:

- Damage and phase-field presented satisfactory results when applied as transition variables, both to represent the structural behavior via equilibrium path and the explicit crack from nodal duplication;
- The crack opening limit for damage is the interval of $[0.8, 0.99]$ to damage and $[0.9, 1.0]$ to phase-field.
- About the spontaneous nucleation, damage and phase-field reproduced the experimental curve properly;
- Damage better represented the discrete crack than the phase-field in the nucleation analysis. The crack deviation observed for phase-field can be related to the element that remains connecting the crack surfaces, preventing it from propagating correctly. A possible solution is coupling nodal duplication algorithm and erosion strategy [24].
- More tests are required to extend these conclusions from the L-shaped panel to general structures using different structural geometries and boundary conditions.

Acknowledgements. The authors gratefully acknowledge the support of the Brazilian research agency CNPq (in Portuguese *Conselho Nacional de Desenvolvimento Cientfico e Tecnológico*) for the PhD Scholarship and the Research Grant n. 307985/2020-2.

Authorship statement. The authors hereby confirm that they are the sole liable persons responsible for the authorship of this work, and that all material that has been herein included as part of the present paper is either the property (and authorship) of the authors, or has the permission of the owners to be included here.

References

[1] J. Janson and J. Hult. Fracture mechanics and damage mechanics - a combined approach. *J. de Méc. Appl.*, vol. 1, n. 1, pp. 69–84, 1977.
[2] D. Legendre and J. Mazars. Damage and fracture mechanics for concrete (a combined approach). In S. V. S.R. Taplin, D.M.R. Rao, P. Rama, J.F. Knott, R. Dubey, ed, *Advances in fracture research: proceedings of the 6th International Conference on Fracture (ICF6)*, volume 4, pp. 2841–2848, New Delhi, India, 1984.
[3] J. Mazars and G. Pijaudier-Cabot. From damage to fracture mechanics and conversely: A combined approach. *Int. J. Solids Struct.*, vol. 33, n. 20-22, pp. 3327–3342, 1996.
[4] M. Jirásek and T. Zimmermann. Embedded crack model. Part II. Combination with smeared cracks. *Int. J. Numer. Methods Eng.*, vol. 50, n. 6, pp. 1291–1305, 2001.
[5] A. Simone, G. N. Wells, and L. J. Sluys. From continuous to discontinuous failure in a gradiente-enhanced continuum damage model. *Comput. Methods Appl. Mech. Eng.*, vol. 192, pp. 4581–4607, 2003.
[6] C. Comi, S. Mariani, and U. Perego. An extended fe strategy for transition from continuum damage to mode i cohesive crack propagation. *Int. J. Numer. Anal. Methods Geomech.*, vol. 31, pp. 213–238, 2007.
[7] P. Moonen, J. Cameliet, and L. Sluys. A continuous-discontinuous approach to simulate fracture processes in quasi-brittle materials. *Philos. Mag.*, vol. 88, n. 28-29, pp. 3281–3298, 2008.
[8] A. Karamnejad, V. P. Nguyen, and L. J. Sluys. A multi-scale rate dependent crack model for quasi-brittle heterogeneous materials. *Eng. Fract. Mech.*, vol. 104, pp. 96–113, 2013.
[9] S. N. Roth, P. Léger, and A. Soulaïmani. A combined XFEM-damage mechanics approach for concrete crack propagation. *Comput. Methods Appl. Mech. Eng.*, vol. 283, pp. 923–955, 2015.
[10] B. Giovanardi, A. Scotti, and L. Fomaggia. A hybrid xfem - phase field (xfield) method for crack propagation in brittle elastic materials. *Comput. Methods Appl. Mech. Eng.*, vol. 320, pp. 396–420, 2017.
[11] R. J. M. Geelen, Y. Liu, J. E. Dolbow, and A. Rodriguez-Ferran. An optimization-based phase-field method for continuous-discontinuous crack propagation. *Int. J. Numer. Methods Eng.*, vol. 116, pp. 1–20, 2018.
[12] T. Rabczuk. Computational methods for fracture in brittle and quasi-brittle solids: state-of-the-art review and future perpectives. *Int. Sch. Res. Notices*, vol. 2013, n. ID 849231, pp. 1–38, 2013.
[13] J. Y. Wu, V. P. Nguyen, C. T. Nguyen, D. Sutula, S. Sinaie, and S. Bordas. Phase-field modeling of fracture. *Adv. Appl. Mech.*, vol. 53, in press, 2019.
[14] de J. H. Vree, W. A. M. Brekelmans, and van M. A. J. Gils. Comparison of nonlocal approaches in continuum damage mechanics. *Comput. Struct.*, vol. 55, n. 4, pp. 581–588, 1995.
[15] L. R. S. Pereira and S. S. Penna. A continuous-discontinuous strategy to represent the crack process in concrete structures. *Proceedings of the XLIII Ibero-Latin-American Congress on Computational Methods in Engineering, CILAMCE*, 2022.
[16] C. Miehe, F. Welschinger, and M. Hofacker. Thermodynamically consistent phase-field models of fracture: Variational principles and multi-field FE implementations. *Int. J. Numer. Methods Eng.*, vol. 83, pp. 1273–1311, 2010a.
[17] C. Miehe, M. Hofacker, and F. Welschinger. A phase field model for rate-independent crack propagation: Robust algorithmic implementation based on operator splits. *Comput. Methods Appl. Mech. Eng.*, vol. 199, pp. 2765–2778, 2010b.
[18] J. Mediavilla, R. H. J. Peerlings, and M. G. D. Geers. A robust and consistent remeshing-transfer operator for ductile fracture simulations. *Computers and Structures*, vol. 84, pp. 604–623, 2006.
[19] S. Cuvilliez, F. Feyel, E. Lorentz, and S. Michel-Ponelle. A finite element approach coupling a continuous gradient damage model and a cohesive zone model within the framework of quasi-brittle failure. *Comput. Methods Appl. Mech. Eng.*, vol. 237-240, pp. 244–259, 2012.
[20] B. Winkler, G. Hofstetter, and G. Niederwanger. Experimental verification of a constitutive model for concrete cracking. In *Proceedings of the Institution of Mechanical Engineers, Part L. Journal of Materials: Design and Applications*, pp. 75–86, 2001.
[21] B. Winkler, G. Hofstetter, and H. Lehar. Application of a constitutive model for concrete to the analysis of a precast segmental tunnel lining. *Int. J. Numer. Anal. Methods Geomech.*, vol. 28, pp. 797–819, 2004.
[22] B. Bourdin, G. A. Fracfort, and J.-J. Marigo. Numerical experiments in revisited brittle fracture. *J. Mech. Phys. Solids*, vol. 48, pp. 797–826, 2000.
[23] J. L. Batoz and G. Dhat. Incremental displacement algorithms for nonlinear problems. *Int. J. Numer. Methods Eng.*, vol. 14, pp. 1262–1267, 1979.
[24] B. M. Luccioni, G. F. Araóz, and N. A. Labanda. Defining erosion limit for concrete. *Int. J. Prot. Struct.*, vol. 4, n. 3, pp. 315–339, 2013.